

Confined photon modes with triangular symmetry in hexagonal microcavities in 2D photonic Crystals

Yuriy A. Kosevich*

*Wave Phenomena Group, Department of Electronic Engineering,
Polytechnic University of Valencia, c/Camino de Vera s/n, E-46022 Valencia, Spain*

José Sánchez-Dehesa†

*Wave Phenomena Group, Nanophotonics Technology Center,
Polytechnic University of Valencia, c/Camino de Vera s/n, E-46022 Valencia, Spain*

Alfonso R. Alija and Luis J. Martínez

*Instituto de Microelectrónica de Madrid,
Centro Nacional de Microelectrónica,
Consejo Superior de Investigacion Científicas,*

Isaac Newton 8, PTM Tres Cantos, 28760 Madrid, Spain

María L. Dotor and Pablo A. Postigo

*Instituto de Microelectrónica de Madrid,
Centro Nacional de Microelectrónica,
Consejo Superior de Investigaciones Científicas,
Isaac Newton 8, PTM Tres Cantos, 28760 Madrid, Spain*

Dolores Golmayo

*Instituto de Ciencia de Materiales,
Consejo Superior de Investigacion Científicas, Cantoblanco, 28049 Madrid, Spain*

(Dated: May 26, 2019)

Abstract

We present the theoretical and experimental studies of the size and thickness dependencies of the optical emission spectra from microcavities with hexagonal shape in films of two-dimensional photonic crystal. A semiclassical plane-wave model is developed to predict the eigenfrequencies of the confined photon modes as a function of both the hexagon-cavity size and film thickness. Modes with two different symmetries, triangular and hexagonal, are considered. It is shown that the model of confined photon modes with triangular symmetry gives an excellent agreement between the predicted eigenmodes and the observed spontaneous emission peaks. Also, we present a comparison between the models of the triangular- and hexagonal-symmetry confined photon modes with the observed resonances, which shows a better agreement with the model based on triangular-symmetry modes.

PACS numbers: 42.70.QS, 78.55.-m, 42.25.Fx, 87.64.Xx

I. INTRODUCTION

New physics often emerges in confined systems when reduced dimensionality leads to new symmetries that, together with the confinement, result in new interesting phenomena. Microcavities in two-dimensional photonic crystals (2D PhCs) are an important example of actual confining structures. They are used for localization of photons into PhC bandgaps (BGs) in order to build ultra-small, low-loss, low-power and low-threshold lasers and light-emitting structures¹. In recent years an important amount of research, both fundamental and applied, has been focused on PhCs microcavities with hexagonal shape fabricated in semiconductor slabs perforated with holes, see, e.g.,^{2,3}, the vertical emission and lasing from which have been successfully demonstrated^{4,5,6}. In such microcavities, the light waves having frequencies inside the photonic bandgap can be considered as circulating around the perimeter of the cavity due to multiple total internal reflections at its boundary.⁷. Vertical emission and lasing from such microcavities can be achieved by the coupling of the confined phonon modes (with TE polarization) to the vacuum states. Similar “vertically emitting” 2D systems are also realized in live nature, for example in fluorescent butterfly wing scales⁸.

The eigenfrequencies of the confined photon modes are among most important characteristics of a microcavity: they determine the energies of photons having maximal spontaneous emission probabilities (the Purcell effect). In this work we present both theoretical and experimental arguments in favor of the existence of two degenerate photon eigenmodes with *triangular symmetry* in hexagonal microcavities. A semiclassical plane-wave model is developed to predict the eigenfrequencies of the confined photon modes as a function both of the hexagon-cavity size and film thickness. We show that the eigenfrequencies of the triangular-symmetry modes determine spectral positions of spontaneous emission peaks, which were recently observed in photoluminescence spectra from microcavities in a 2D PhC in III-V semiconductor slabs [9]. Here, a new set of microcavities has been built and characterized. As in Ref. [9], by accurate changing the PhC film thickness the wavelengths of the PhC microcavity eigenmodes are tuned in order of tens of nanometers toward higher energies. A comparison of the observed eigenmodes with the spectral positions predicted by the models of the modes with triangular symmetry and hexagonal symmetry has also been performed. From that comparison we conclude that for the higher wavenumber (in microcavities with larger lateral size) the proposed model of triangular-symmetry modes gives better agreement

with the experiment in comparison with the model of hexagonal-symmetry modes. Therefore we expect that the proposed model of triangular-symmetry modes will be useful both in understanding the physical origin and for the quantitative prediction of the spontaneous emission peaks in 2D PhC microcavities in the form of ideal and distorted hexagons.

II. EXPERIMENTAL SETUP

Experimentally, several 2D PhC structures with a hexagonal lattice of circular air holes have been fabricated in an InGaAsP semiconductor film incorporating an active medium composed of three $\text{In}_{0.47}\text{Ga}_{0.53}\text{As}$ quantum wells. This structure gives rise to strong photoluminescence (PL) spectra centered around 1500 nm at room temperature. Processing of the PhC structures was done by electron-beam lithography of a poly(methyl methacrylate) (PMMA) layer on top of a SiO_2 layer (120 nm thick)⁹. To provide the membranes with sufficiently strong mechanical support, the fabricated layers were bonded to a thin borosilicate glass ($n = 1.53$) with optical glue ($n = 1.5$). Circular holes were made in the InGaAsP membrane by reactive ion beam etching. A 2D hexagonal PhC array with lattice constant $a = 500$ nm surrounds hexagonal microcavities with a variable number of missing holes per side. Here, H3 (three missing holes per side) and H5 (three missing holes per side) microcavities are fabricated and characterized. Figure 1 shows a scanning electron microscopy image of one H5 microcavity and a descriptive drawing of the fabricated structure. Different values of the radius of the holes r around $0.33a$ have been used. The variation of the radius r is estimated from the scanning electron microscopy pictures, being below 5%. With this choice of parameters, a large band gap exists for the TE mode between the normalized frequencies of $\omega a/(2\pi c) \sim 0.28$ and $\omega a/(2\pi c) \sim 0.36$, which corresponds to the wavelength range of 1250-1600 nm. The fabricated structures are optically pumped with a 780 nm laser diode. An objective lens (0.40 NA) is used to focus the excitation spot. The size of the excitation spot was around $3.5 \mu\text{m}$ which is small enough to fit inside the PC structures and to generate cavity modes. Light is collected by a lens inside a 0.22 m monochromator with a cooled InGaAs photodiode connected to a lock-in amplifier. The resolution of the experimental setup in this configuration is around 2.5 nm.

III. MODEL

Now we turn to the description of our model. Figure 2(a) shows the hexagonal cavity and the ray paths, which belong to the two degenerate triangular-symmetry modes. Within the semiclassical plane-wave model, the dispersion equation for the degenerate triangular-symmetry photon modes, confined in an ideal hexagonal microcavity in 2D PhC, can be obtained from the requirement that the total phase shift of the wave along its closed path is an integer multiple of 2π :

$$k_i^{(N)} 4.5R - 3\phi = 2\pi N, \quad (1)$$

$$\frac{\omega_N}{2\pi} = \frac{c_i}{\lambda_i^{(N)}} = \frac{c}{4.5Rn_{eff}} \left(N + \frac{3\phi}{2\pi} \right), \quad (2)$$

where N is integer “quantum” wavenumber, ϕ takes into account the additional phase shift that occurs during the total internal reflection of the confined photon mode in the 2D PhC bandgap frequency region, c_i and $k_i = 2\pi/\lambda_i$ are, respectively, the wave velocity and the *in-plane* wave-vector inside the cavity. It will be shown below that the corresponding wavenumbers N in the considered H3 and H5 microcavities are rather large, $N \gg 1$, which justifies the use of the semiclassical plane-wave model in resolving the eigenfrequencies.

We assume that in (or close to) the middle of the PhC bandgap the additional phase shift ϕ in Eqs. (1) and (2) is equal to the Keller additional phase shift due to leakage of (electron) wavefunction into classically forbidden regions, $\phi = \frac{\pi}{2}$, see Refs. [10]. In the middle of the PhC BG, the phase shift 3ϕ does not depend on the exact form and steepness of the effective confining potential, is independent of wavenumber N and depends only on the number of turning points (equal to 3 or 6 for the triangular- or hexagonal-symmetry modes, respectively, see Figs. 2(a) and 2(b)). It is worth mentioning that we assume that in the middle of the BG the additional phase shift $\phi = \frac{\pi}{2}$ in Eqs. (1) and (2) is fixed and does not explicitly depend on the phase of the coefficient of the total internal reflection of the confined photon modes, in contrast to the similar to Eqs. (1) and (2) semiclassical plane-wave model which was applied to the total-internal-reflection dielectric microresonators with hexagonal cross section, see Ref. [11]. The point is that the phase of the coefficient of the total internal reflection is different (and the difference is equal to π) for the reflection coefficients of the **E** or **H** fields, which results in different signs of the normal component of the Pointing vector, $\mathbf{P} = \frac{c}{4\pi} \mathbf{E} \times \mathbf{H}$, for the incident and reflected electromagnetic waves, see, e.g., Ref.¹².

Therefore with our choice of ϕ in Eqs. (1) and (2), the wavenumber N is uniquely defined, as in the case of semiclassical Bohr-Sommerfeld quantization condition for the bound electron motion. If we apply the same model to the hexagonal-symmetry photon mode, confined in 2D PhC hexagonal microcavity (in the middle of the PhC BG), see Fig. 2(b), $4.5R$ and 3ϕ in l.h.s. of Eq. (1) and r.h.s. of Eq. (2) should be replaced, respectively, by $3\sqrt{3}R$ and 6ϕ , with $\phi = \frac{\pi}{2}$.

The degeneracy of the two triangular-symmetry modes in an ideal hexagonal microcavity can be removed in a “distorted hexagon”, which is bound by two regular triangles with different sides (see Fig. 2(c)). In this case the total optical paths and correspondingly the eigenfrequencies of the two modes, bound inside the different triangles, will be different.

The cavity eigenfrequencies ω_N in Eq. (2) are determined by the effective refractive index of the system $n_{eff} \equiv c/c_i$. The n_{eff} approach allows us to describe the actual 3D system as an effective 2D system with high accuracy, see, e.g., Ref. [13]. This n_{eff} depends on the polarization of the confined photon mode (TE or TM), and on the relative film thickness $k_id/2\pi = d/\lambda_i$ of the 2D structure. It is possible to obtain an explicit dependence $n_{eff}=n_{eff}(d/\lambda_i)$ by solving dispersion equation for electromagnetic mode in a waveguide formed by a dielectric film with thickness d and dielectric constant ϵ_f , sandwiched between a substrate and a top with dielectric constants ϵ_s and ϵ_t , respectively, see, e.g., Ref.¹⁴. The dispersion equation for the angular frequency ω of TE mode with a given in-plane wave vector k_i in such planar waveguide system has the following form¹⁴:

$$\begin{aligned} \tan \kappa_f d &= \frac{(\kappa_t + \kappa_s)\kappa_f}{\kappa_f^2 - \kappa_t \kappa_s}, \\ \kappa_f &= \sqrt{\frac{\omega^2}{c^2} \epsilon_f - k_i^2}, \quad \kappa_{t,s} = \sqrt{k_i^2 - \frac{\omega^2}{c^2} \epsilon_{t,s}}. \end{aligned} \quad (3)$$

Equation (3) can be cast in the following transcendent equation which relates $\epsilon_{eff}=n_{eff}^2$, $\epsilon_f > \epsilon_{eff} > (\epsilon_t, \epsilon_s)$, with the dimensionless in-plane wavenumber k_id :

$$\begin{aligned} \tan \left[k_id \sqrt{\frac{\epsilon_f}{\epsilon_{eff}} - 1} \right] &= \\ \left[\sqrt{1 - \frac{\epsilon_s}{\epsilon_{eff}}} + \sqrt{1 - \frac{\epsilon_t}{\epsilon_{eff}}} \right] \sqrt{\frac{\epsilon_f}{\epsilon_{eff}} - 1} & \\ \frac{\epsilon_f}{\epsilon_{eff}} - 1 - \sqrt{1 - \frac{\epsilon_s}{\epsilon_{eff}}} \sqrt{1 - \frac{\epsilon_t}{\epsilon_{eff}}} &. \end{aligned} \quad (4)$$

Figure 3 presents a numerical solution of Eq. (4) for the TE_0 mode for n_{eff} as a function of d/λ_i (in the interval of interest for our microcavities) in a InGaAsP planar waveguide bonded

on a SiO_2 substrate, and using air as top layer. Figure 3 shows that n_{eff} is a monotonously increasing function of d/λ_i , which can be explained by the stronger confinement inside the high-index InP layer of the cavity modes with the smaller, with respect to the layer thickness, wavelengths. Qualitatively similar dependence of n_{eff} on d in a 2D PhC system was previously obtained in Ref. [15] by numerical evaluation of the space-averaged electric-field mode energy.

IV. RESULTS AND DISCUSSION

The d/λ_i -dependence of n_{eff} in Eq. (2) furnishes the clue to a quantitative description within the proposed model of the observed d -dependence of the microcavity eigenfrequencies. To describe the predicted eigenfrequencies (emission peaks) in the measured optical spectra, see Fig. 4, we use $R = 5a$ and $R = 3a$ as the side lengths of the H5 and H3 microcavities in Eqs. (1) and (2). Symbols in Fig. 5 show the spectral positions of the observed absolute eigenfrequencies (in reduced units), $\omega_{\text{Na}}/2\pi c$, as a function of the InGaAsP film thickness (d), while solid (dashed) lines give the predicted by Eqs. (1) - (4) eigenfrequencies of the confined triangular-symmetry (hexagonal-symmetry) photon modes, without any fitting parameters.

Within the model of triangular-symmetry modes, $N = 19$, $N = 20$ and $N = 21$ correspond, respectively, to the 1st, 2nd and 3rd peak in the H5 cavity, and $N = 11$ and $N = 12$ correspond to the 1st and 2nd peak in the H3 cavity. (Within the model of hexagonal-symmetry modes, $N_{\text{hex}} = 21$, $N_{\text{hex}} = 22$ and $N_{\text{hex}} = 23$ correspond, respectively, to the 1st, 2nd and 3rd peak in the H5 cavity, and $N_{\text{hex}} = 11$ and $N_{\text{hex}} = 12$ correspond to the 1st and 2nd peak in the H3 cavity.) The corresponding wavenumbers N (and N_{hex}) are indeed large, as it was mentioned above. The best agreement of the model of triangular-symmetry modes with the measurements is reached for the half-wavelength layer, $d = 235 \text{ nm} \approx \lambda/2n_f$, λ being the vacuum wavelength. In this case the wave path is indeed close to the two-dimensional path in the plane of the microcavity, while the path becomes more three-dimensional for the larger slab thicknesses. As it is seen in Fig. 5, the model of triangular-symmetry modes describes better, in comparison with the model of hexagonal-symmetry modes, the absolute eigenfrequencies of the observed confined modes with higher wavenumber N (in microcavities with larger lateral size), as one should expect for the semiclassical model. On the other

hand, the only two observed strong emission peaks in H3 microcavities, in contrast to three strong peaks in H5 microcavities, cf. Figs. 4(a) and 4(b), do not allow a definitive selection between the models of triangular- and hexagonal-symmetry modes in H3 microcavities.

Figure 6 shows dimensionless eigenfrequencies $\omega a n_{eff} / 2\pi c = a / \lambda_i$ with corresponding wavenumbers N and N_{hex} (for the triangular- and hexagonal-symmetry modes, respectively) versus InGaAsP layer thickness. Now, solid (dashed) lines represent the constant values predicted by Eq. (2) for the confined triangular-symmetry (hexagonal-symmetry) modes, and different bold symbols define the peaks in the optical spectra (not shown) measured in a new set of H5 and H3 fabricated microcavities. To include the experimental data in Fig. 6, we have used Eq. (4) [for the same $n_{eff}(d/\lambda_i^{(N)})$ as in Fig. 5]. The agreement found with the new data supports our model of triangular-symmetry modes. At this point, let us remember that dielectric microresonators and microcavities with hexagonal shape, which are often called as whispering-gallery resonators, have also attracted much interest for possible optical applications in recent years. The whispering-gallery modes in dielectric resonators correspond to the hexagonal-symmetry modes in hexagonal microcavities in 2D PhC (see Fig. 2(b)). From such dielectric microresonators, the “horizontal” emission is achieved by the coupling of the vacuum states to the confined phonon modes with TM polarization. Recent studies of dielectric microresonators made of zinc oxide (ZnO) nanoneedles with hexagonal cross section have been reported¹¹. A model of triangular-symmetry modes can also be applied to such dielectric microresonators. The refractive index of ZnO is close to 2 and, therefore, the critical angle of incidence for total internal reflection is close to $\pi/6$. Since the angle of incidence of triangular-symmetry (whispering-gallery) modes in a microresonator with hexagonal shape is $\pi/6$ ($\pi/3$), see Figs. 2(a) and 2(b), the triangular-symmetry modes in such dielectric microresonators can be considered as *radiating* counterparts of *non-radiating* whispering-gallery modes.

V. SUMMARY

In summary, we show that confined degenerate photon eigenmodes with triangular symmetry can be the origin of the emission peaks observed in the optical spectra from hexagonal microcavities in 2D photonic crystals. An analytical semiclassical plane-wave model has been developed for the quantitative evaluation of the eigenfrequencies of those photon modes lo-

calized due to total internal reflection. The analytical model describes quantitatively both the experimentally observed cavity-size and photonic-crystal-thickness dependencies of the frequencies of the confined eigenmodes. Removal of the degeneracy and change of eigenfrequencies of confined photon modes are predicted for microcavities in the form of distorted hexagon.

VI. ACKNOWLEDGEMENTS

Work supported by Ministry of Science and Education (MEC) of Spain (Refs. TEC2004-03545, TEC2005-05781-C03-01, NAN2004-08843-C05-04, NAN2004-09109-C04-01), and contracts S-505/ESP/000200, UE NoEs SANDIE (NMP4-CT-2004-500101) and PHORE-MOST (IST-2-511616-NOE). The authors acknowledge useful discussions with Andreas Håkansson, Javier Martí and Daniel Torrent. Yu. A. K. acknowledges a support from MEC (Grant SAB2004-0166). A. R. A. thanks a FPU fellowship (Ref. AP2002-0474) and L. J. M. an I3P fellowship.

* Permanent address: Semenov Institute of Chemical Physics, Russian Academy of Sciences, ul. Kosygina 4, 119991 Moscow, Russia.

† jsdehesa@upvnet.upv.es

- ¹ For recent reviews see S. Noda, *Science*, **284**, 1819 (2006); K. Vahala, *Nature (London)*, **432**, 839 (2003).
- ² S. Noda and T. Baba, *Roadmap on Photonic Crystals* (Kluwer Academic Publishers, Dordrecht, 2003).
- ³ Jean-Michel Lourtioz, Henri Benisty, Vincent Berger, Jean-Michel Gérard, Daniel Maystre, and Alexis Tchelnokov, *Photonic Crystals: Towards Nanoscale Photonic Devices* (Springer-Verlag, Berlin, 2005).
- ⁴ O. Painter, R.K. Lee, A. Sherer, A. Yariv, J.D. O'Brien, P.D. Dapkus, and I.Kim, *Science*, **284**, 1819 (1999).
- ⁵ H-G. Park, S.-H. Kim, S.H. Kwon, Y.G. Ju, J.K. Yang, J.H. Baek, S.B. Kim, and Y.H.Lee, *Science*, **305**, 1444 (2004).
- ⁶ M. Fujita, S. Takahashi, Y. Tanaka, T. Asano, and S. Noda, *Science*, **308**, 1296 (2005).
- ⁷ P. Pottier, C. Seassal, X. Letartre, J.L. Leclercq, P. Viktorovitch, D. Cassagne, and C. Joannin, *J. Lightwave Technol.* **17**, 2058 (1999).
- ⁸ P. Vukusic and I. Hooper, *Science*, **310**, 1151 (2005).
- ⁹ A. R. Alija, L. J. Martinez, A. Garcia-Martin, M. L. Dotor, D. Golmayo, and P. A. Postigo, *Appl. Phys. Lett.* **86**, 141101 (2005).
- ¹⁰ J. B. Keller, *Ann. Phys. (NY)* **4**, 180 (1958); A. D. Stone, *Phys. Today* **58**, No. 8, 37 (2005).
- ¹¹ Th. Nobis, E. M. Kaidashev, A. Rahm, M. Lorenz, and M. Grundmann, *Phys. Rev. Lett.* **93**, 103903 (2004).
- ¹² L. D. Landau and E. M. Lifshitz, *Electrodynamics of Continuous Media* (Butterworth-Heinemann, Oxford, 1984).
- ¹³ M. Qiu, *Appl. Phys. Lett.* **81**, 1163 (2002).
- ¹⁴ H. A. Haus, *Waves and Fields in Optoelectronics* (Prentice-Hall, New Jersey, 1984).
- ¹⁵ H. Y. Ryu, J. K. Hwang, and Y. H. Lee, *IEEE J. Quantum Electron.*, **39**, 314 (2003).

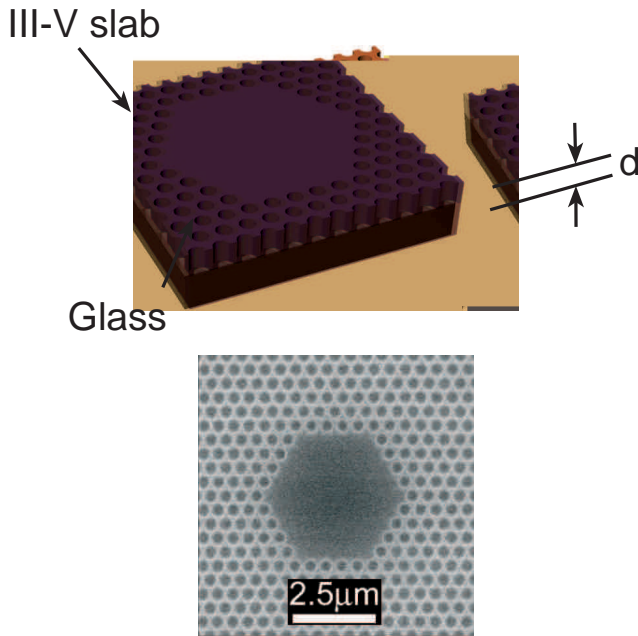


FIG. 1: (Lower image) Scanning electron microscopy image of the fabricated H5 cavities. (Upper image) Schematic view of H5 microcavity fabricated on the III-V semiconductor slab with a thickness $d=265$ nm bonded to a glass substrate.

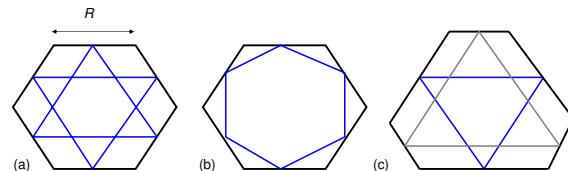


FIG. 2: (color online) Ray paths in triangular-symmetry modes in ideal, (a), and distorted, (c), hexagons; (b) presents ray path for the hexagonal-symmetry mode in an ideal hexagon. Two triangular-symmetry modes are degenerate in an ideal hexagon, and have different optical paths and eigenfrequencies in a distorted hexagon.

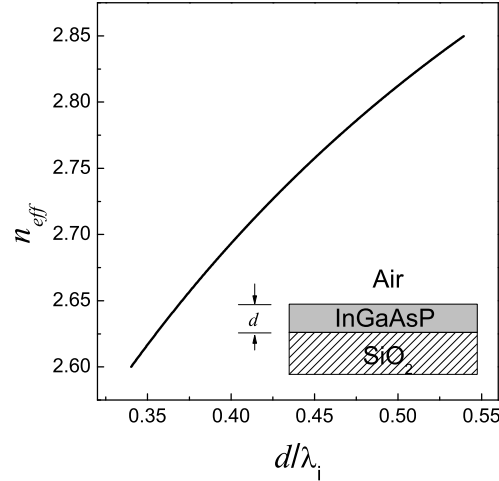


FIG. 3: Effective refractive index n_{eff} versus InGaAsP layer thickness over internal wavelength d/λ_i in a planar waveguide with $\epsilon_f = 10.89$ (InGaAsP), $\epsilon_s = 2.34$ (SiO_2) and $\epsilon_t = 1$ (air).

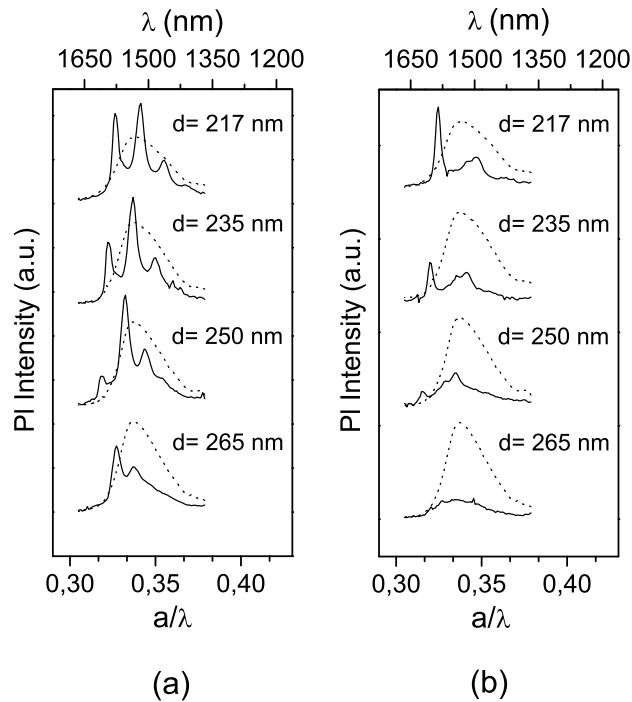


FIG. 4: Photoluminescence spectra of the H5 (a) and H3 (b) microcavities with different slab thicknesses d (solid lines). The spectra of an unpatterned region in the vicinity of the microcavity is also shown (dotted lines). Here λ is the vacuum wavelength: $a/\lambda = \omega a/2\pi c$.

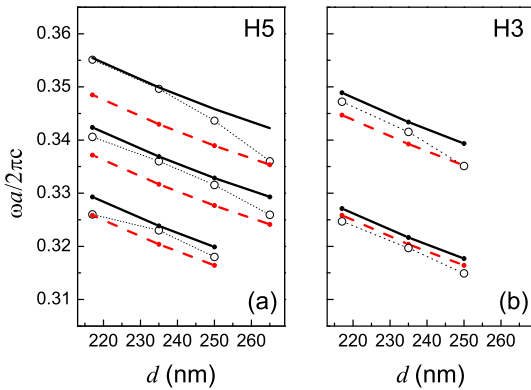


FIG. 5: (color online) Normalized frequencies of emission peaks produced by localized modes in H5 (a) and H3 (b) microcavities as a function of InP layer thickness, d . Open circles represent the experimental data obtained by microphotoluminescence. The dotted lines are guides for the eye. Solid (red dashed) lines show the theoretical prediction given by the model of confined triangular-symmetry (hexagonal-symmetry) modes.

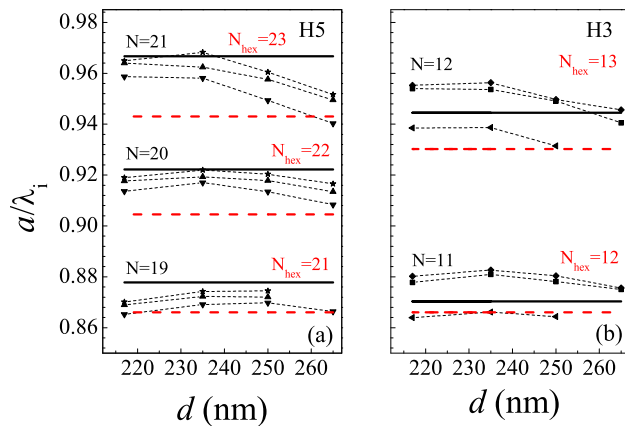


FIG. 6: (color online) Normalized eigenfrequencies with corresponding wavenumbers N and N_{hex} (for the triangular- and hexagonal-symmetry modes, respectively) of emission peaks produced by confined photon modes in H5 (a) and H3 (b) microcavities as a function of InP layer thickness d . Different bold symbols represent the experimental data obtained by microphotoluminescence. Solid (red dashed) lines represent the theoretical prediction given by the model of confined triangular-symmetry (hexagonal-symmetry) modes.